Transformation of a Methyleneamide Ligand at Molybdenum: Electrochemical Oxidation to a Cyanide, Reactions with Elemental Oxygen, Sulphur or Selenium and X-Ray Crystal Structures of *trans*-[Mo(CN)Cl(dppe)$_2$]·MeOH and *trans*-[Mo(NCS)Cl(dppe)$_2$];† Electroreduction of the Cyanide to an Aminocarbyne, *trans*-[Mo(CNH$_2$)Cl(dppe)$_2$] (dppe = Ph$_2$PCH$_2$CH$_2$PPh$_2$)

Adrian Hills, David L. Hughes, Colin J. Macdonald, Modher Y. Mohammed and Christopher J. Pickett*

AFRC Institute of Plant Science Research, Nitrogen Fixation Laboratory, University of Sussex, Brighton BN1 9RQ, UK

Deprotonation of the methylimide *trans*-[Mo(NMe)Cl(dppe)$_2$]$^+$ (dppe = Ph$_2$PCH$_2$CH$_2$PPh$_2$) gives the reactive methyleneamide *trans*-[Mo(NCH$_2$)Cl(dppe)$_2$] **A**; oxidation of **A** at a platinum anode or by iodine gives *trans*-[Mo(CN)Cl(dppe)$_2$] **B**, the structure of which has been determined by X-ray crystallography. Carbon-13 labelling studies suggest that the rearrangement of the MoNC framework to MoCN is intramolecular. Compound **A** reacts with chalcogens to give heterocumulene complexes *trans*-[Mo(NCX)Cl(dppe)$_2$] **C** (X = O, S or Se), and the X-ray crystal structure of the sulphur derivative shows that the NCS ligand is N-bonded as an isothiocyanate. The electrochemistry of compound **B** is extensive: reduction under N$_2$ gives *trans*-[Mo(N$_2$)(CN)(dppe)$_2$]$^-$ and in the presence of phenol affords the isolable aminocarbyne *trans*-[Mo(CNH$_2$)Cl(dppe)$_2$].

The square-planar assembly M(dppe$_2$)$_2$, M = Mo or W, dppe = Ph$_2$PCH$_2$CH$_2$PPh$_2$, provides a robust platform at which N-, O- or C-containing ligands can be electrochemically transformed. For example, hydrazide and dialkylhydrazide ligands can be activated towards protic attack to give ammonia, amines or hydrazines;[1–5] oxides, imides and methylimides can be reduced at a mercury cathode to give dinitrogen complexes and respectively water, ammonia or methylamine;[6–8] a diazenide ligand has been oxidised to a diazoalkane, reaction (1)[9] where M′ = *trans*-Mo(dppe)$_2$, and diazoalkanes reductively C-coupled or reduced to diazenides.[10]

$$[F\text{–}M'\text{–}N{=}N\text{–}CH_2Ph] \xrightarrow[-H^+]{-2e} [F\text{–}M'{=}N\text{–}N{=}CHPh]^+ \quad (1)$$

This paper describes some new electrochemical and chemical transformations of ligands at the Mo(dppe)$_2$ assembly. Some of the reactions described may bear upon both biological reduction of cyanide by nitrogenase and the diversification of the type of nitrogen products that can be synthesised *via* reactions of ligating dinitrogen. Some of this work has been briefly communicated.[11]

Results and Discussion

Synthesis and Characterisation of the Methyleneamide Complex trans-[Mo(NCH$_2$)Cl(dppe)$_2$] **A**.—Deprotonation of the methylimide *trans*-[Mo(NMe)Cl(dppe)$_2$]$^+$ by K[OBu^t] in tetrahydrofuran (thf) gives *trans*-[Mo(NCH$_2$)Cl(dppe)$_2$] **A**, reaction (2), which was isolated as an air-sensitive yellow solid and

$$trans\text{-}[Mo(NMe)Cl(dppe)_2]^+ \underset{+H^+}{\overset{-H^+}{\rightleftharpoons}} trans\text{-}[Mo(NCH_2)Cl(dppe)_2] \quad (2)$$
A

characterised as follows. ^{31}P-{^{1}H} NMR spectroscopy shows a single resonance which demonstrates that the product **A** retains the square-planar array of P atoms about the molybdenum; the relative chemical shifts of the chloro- and bromo-analogues of **A** (^{31}P-{^{1}H}, singlets at δ −83.30 and 86.80 ppm respectively) and of the parent species are consistent with retention of the axial halide ligand. The deprotonation is reversible, treatment of **A** in thf with aqueous HCl regenerating the parent methylimide, reaction (2).

The configuration of the nitrogen ligand in compound **A** as an NCH$_2$ group was established by ^{13}C NMR spectroscopy of the [^{13}C]methyl-labelled derivative. The methylimide shows a quartet, centred at δ 50.4 ppm with $^1J_{CH}$ 150 Hz. This spectrum is replaced on deprotonation by the triplet of the [^{13}C]methylene carbon of **A** at δ 111.4 ppm, $^1J_{CH}$ 181 Hz. Phosphorus-31–carbon-13 coupling was not observed in the NMR spectra of either P or C nuclei and this rules against a sideways-bound NCH$_2$ ligand. Hitherto there has been only one other example of a methyleneamide complex, [Re(NCH$_2$)Cl$_2$(PPh$_3$)$_3$], which was also formed by deprotonation of a methylimide precursor.[12] Substituted alkyleneamido-complexes are well known but none of Mo^{II} or of a type analogous to that reported here.[13]

Anodic and Chemical Oxidation of Complex **A** *to give trans*-[Mo(CN)Cl(dppe)$_2$] **B**: *Alternative Routes to this Product and its Bromo-analogue*.—Cyclic voltammetry shows that the methyleneamide **A** undergoes an irreversible oxidation in thf containing 0.2 mol dm^{-3} [NBu$_4$][BF$_4$] at a platinum electrode

† *trans*-Bis[1,2-bis(diphenylphosphino)ethane-κ^2*P*,*P*′]chlorocyanomolybdenum(II)–methanol (1/1) and bis[1,2-bis(diphenylphosphino)ethane-κ^2*P*,*P*′]chloro(thiocyanate-κ*N*)molybdenum(II).

Supplementary data available: see Instructions for Authors, *J. Chem. Soc., Dalton Trans.*, 1991, Issue 1, pp. xviii–xxii.

Non-SI unit employed: BM ≈ 9.27 × 10^{-24} J T^{-1}.

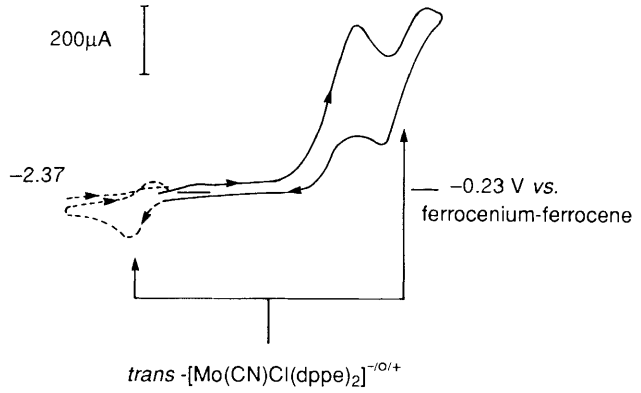

Fig. 1 Oxidation of *trans*-[Mo(NCH$_2$)Cl(dppe)$_2$] formed *in situ* by addition of K[OBu^t] to the methylimide complex. The scan rate was 0.1 V s^{-1} at a platinum-gauze preparative electrode in a thf electrolyte. The irreversible oxidation gives rise to the product oxidation and reduction couples (broken line).

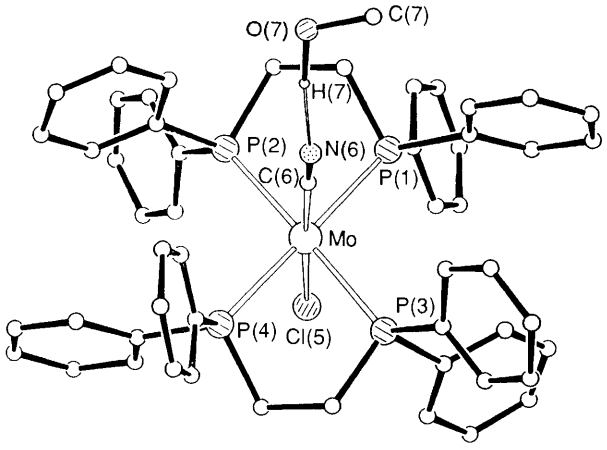

Fig. 2 A view of the X-ray crystal structure of *trans*-[Mo(CN)Cl(dppe)$_2$] showing hydrogen bonding to a methanol solvate

to give a product which both oxidises reversibly and reduces reversibly as shown by Fig. 1. In order to identify the product(s) of oxidation, controlled-potential electrolyses were undertaken on a preparative scale.

Solutions of the methyleneamide were generated *in situ* by addition of K[OBu^t] to *trans*-[Mo(NMe)Cl(dppe)$_2$]$^+$ and oxidation was performed at a potential *ca.* 100 mV positive of E_p for the primary oxidation. The electrolyses at a platinum anode were inefficient in both thf and dimethylformamide (dmf) electrolytes because product(s) fouled the working electrode causing the cell current to die prematurely, see Experimental section. Nevertheless green prisms were isolated on work-up of an anolyte and an X-ray crystallographic analysis of these showed that *trans*-[Mo(CN)Cl(dppe)$_2$] **B** had been synthesised, Fig. 2. Cyclic voltammetry confirmed that the redox chemistry of isolated **B** corresponded to that of the product detected in the voltammetry of **A**, Fig. 1 and reaction (3).

$$\textit{trans}\text{-}[Mo(NCH_2)Cl(dppe)_2] \xrightarrow[-2H^+]{-2e} \underset{\mathbf{B}}{\textit{trans}\text{-}[Mo(CN)Cl(dppe)_2]} \quad (3)$$

The cyanide complex **B** shows a weak IR band at 2056 cm^{-1} which is shifted to 2005 cm^{-1} in the ^{13}C-labelled product; we assign these to ν(C≡N). The complex is both EPR and NMR silent, presumably because it is paramagnetic with two unpaired electrons, as is the closely related compound *trans*-[MoCl$_2$(dppe)$_2$] which has a magnetic moment of 2.89 BM.[14] The crystal structure analysis of the cyanide **B** is described below.

Table 1 Selected molecular dimensions (bond lengths in Å, angles in °) in [Mo(CN)Cl(dppe)$_2$]·MeOH with estimated standard deviations (e.s.d.s) in parentheses

(*a*) About the Mo atom

Mo–P(1)	2.498(1)	Mo–P(4)	2.503(1)
Mo–P(2)	2.509(1)	Mo–Cl(5)	2.432(2)
Mo–P(3)	2.517(1)	Mo–C(6)	2.158(6)
P(1)–Mo–P(2)	79.2*	P(3)–Mo–Cl(5)	83.9*
P(1)–Mo–P(3)	101.7*	P(4)–Mo–Cl(5)	85.9*
P(2)–Mo–P(3)	179.0*	P(1)–Mo–C(6)	82.7(1)
P(1)–Mo–P(4)	176.3(1)	P(2)–Mo–C(6)	86.6(2)
P(2)–Mo–P(4)	99.3*	P(3)–Mo–C(6)	93.0(2)
P(3)–Mo–P(4)	79.8*	P(4)–Mo–C(6)	93.9(1)
P(1)–Mo–Cl(5)	97.5*	Cl(5)–Mo–C(6)	177.0(2)
P(2)–Mo–Cl(5)	96.4*		

(*b*) In the cyanide ligand

C(6)–N(6)	1.061(9)	Mo–C(6)–N(6)	176.8(5)

(*c*) Torsion angles in the dppe ligands

P(1)–C(1)–C(2)–P(2)	44.4(5)	P(3)–C(3)–C(4)–P(4)	−48.1(4)

(*d*) In the methanol molecule and hydrogen bonds

C(7)–O(7)	1.380(14)	C(7)–O(7)–H(7)	112(4)
O(7)–H(7)	1.24(9)	C(7)–O(7)···N(6)	107.6(6)
O(7)···N(6)	2.838(9)	O(7)–H(7)···N(6)	173(6)
H(7)···N(6)	1.60(9)		

* E.s.d. is less than 0.05°.

Because the electrosynthesis of the cyanide **B** was inefficient, we looked for other ways to synthesise it and found two routes. *In situ* generation of the methyleneamide in thf in the presence of excess of the butoxide followed by addition of iodine gave the cyanide in good yield, reaction (4). The rearrangement of the

$$\textit{trans}\text{-}[Mo(NMe)Cl(dppe)_2]^+ \xrightarrow[(ii)I_2\text{–thf}]{(i)K[OBu^t]\text{–thf}} \underset{\mathbf{B}}{\textit{trans}\text{-}[Mo(CN)Cl(dppe)_2]} \quad (4)$$

MoNC framework to MoCN is probably an intramolecular process: iodine oxidation of ^{13}C-labelled **A** in the presence of an excess of [NBu$_4$][^{12}CN] in thf showed no evidence for the incorporation of the [^{12}C]cyanide label by IR spectroscopy. The second chemical route is particularly convenient because compound **B** can be synthesised in a one-pot reaction from *trans*-[Mo(N$_2$)$_2$(dppe)$_2$] in excellent yield, *via* the formation of *trans*-[Mo(N$_2$)(CN)(dppe)$_2$]$^-$ as outlined in reaction (5) and described in the Experimental section. The pathway of

$$\textit{trans}\text{-}[Mo(N_2)_2(dppe)_2] \xrightarrow[(ii)PhCH_2Cl]{(i)[NBu_4][CN]\text{–thf}} \underset{\mathbf{B}}{\textit{trans}\text{-}[Mo(CN)Cl(dppe)_2]} \quad (5)$$

this reaction undoubtedly parallels that for formation of *trans*-[MoCl$_2$(dppe)$_2$] from benzyl chloride and *trans*-[Mo(N$_2$)$_2$(dppe)$_2$].[14] The bromo-analogue of **B** has been synthesised, see Experimental section.

X-Ray Crystal Structure of trans-[Mo(CN)Cl(dppe)$_2$]·MeOH: *Description of the Molecule*.—The *trans*-[Mo(CN)Cl(dppe)$_2$] molecule shows octahedral co-ordination of the Mo atom, with four P atoms forming a good equatorial plane and the Cl–Mo–C–N moiety in almost linear array nearly normal to that plane, Fig. 2. The Mo atom is displaced slightly (0.04 Å) from the equatorial plane towards the chloride ligand. The two diphosphine ligands show an almost perfect centrosymmetric

Table 2 Primary redox potentials[a] of molybdenum(II) compounds

Complex	Primary reduction (Mo^{II}–Mo^{I}) $E_{\frac{1}{2}}^{red}$/V	Primary oxidation (Mo^{II}–Mo^{III}) $E_{\frac{1}{2}}^{ox}$/V	ΔE^b/V
trans-[Mo(NCH$_2$)Cl(dppe)$_2$]	−3.11[c]	−0.72	2.34
trans-[Mo(OH)Cl(dppe)$_2$][d]	−2.62[c]	−1.10[c]	1.52
trans-[Mo(NH$_2$)Cl(dppe)$_2$][d]	−2.60[c]	−1.51	1.09
trans-[MoCl$_2$(dppe)$_2$]	−2.22	−0.59	1.63
trans-[Mo(NCO)Cl(dppe)$_2$]	−2.16	−0.53	1.63
trans-[Mo(NCS)Cl(dppe)$_2$]	−1.96	−0.44	1.52
trans-[Mo(NCSe)Cl(dppe)$_2$]	−1.92	−0.40	1.52
trans-[Mo(CN)Cl(dppe)$_2$]	−1.76	−0.45	1.31

[a] Relative to ferrocenium–ferrocene. [b] Separation of oxidation and reduction potentials, a measure of the difference of HOMO and lowest unoccupied molecular orbital energy levels. The horizontal line between the amido- and dichloro-complexes defines the two classifications discussed in the text: complexes above the line are in group (*i*), below in group (*ii*). [c] Process is irreversible, values given are for peak potentials, E_p. [d] Species not isolated; values are for electrogenerated intermediates, see refs. 6 and 7.

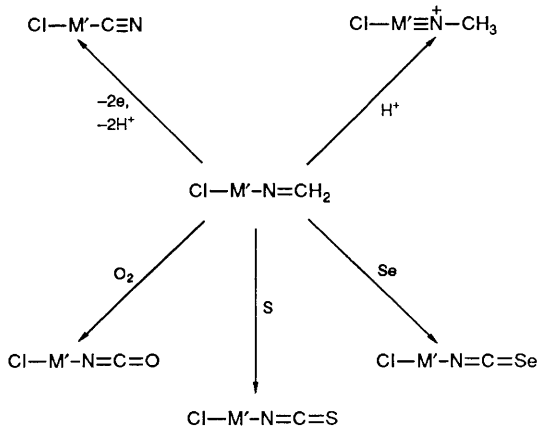

Scheme 1 M′ = Mo(dppe)$_2$

arrangement, with the P–C–C–P linkages having typical *gauche* conformations with torsion angles of 44.4(5) and −48.1(4)°. The Mo–Cl distance of 2.432(2) Å is normal for Mo^{II} in octahedral co-ordination. This is the first recorded example of a cyanide group ligating Mo in a phosphine environment; dimensions are in Table 1.

The hydroxyl hydrogen atom of the solvent methanol molecule was located and refined satisfactorily. The O–H distance appears rather long, 1.24(9) Å, but H(7) is pointing directly towards N(6) with the H • • • N distance 1.60(9) Å. The methanol molecule is thus linked to the cyanide ligand through a strong hydrogen bond. All other contacts between molecules are by normal van der Waals interactions.

Synthesis of Isocyanate, Isothiocyanate and Isoselenocyanate Complexes.—We noticed that the methyleneamide complex was air sensitive and exposure of Nujol mulls of **A** to air gave rise to a sharp IR band at 2200 cm^{-1} which is characteristic of an isocyanate. We therefore examined the oxygenation of solutions of **A** and found that a bright yellow isocyanate complex *trans*-[Mo(NCO)Cl(dppe)$_2$] **C** was isolable in moderate yield as described in the Experimental section, reaction (6). The

$$\textit{trans}\text{-}[Mo(NMe)Cl(dppe)_2]^+ \xrightarrow[(ii)O_2\text{-thf}]{(i)K[OBu^t]\text{-thf}} \textit{trans}\text{-}[Mo(NCO)Cl(dppe)_2] \quad (6)$$

C

oxygenation also produced a small amount of the less soluble cyanide **B** which could be removed by recrystallisation from thf.

The IR band for ν(NCO) at 2200 cm^{-1} shifts to 2150 cm^{-1} for the ^{13}C-labelled complex. It is difficult to distinguish between N- and O-bonded isocyanates on the basis of ν(NCO) stretching frequences.[15,16] However there are very few reported cyanato-*O* complexes and none whose structure has been confirmed by X-ray crystallography. Only one complex [Ti(η^5-C$_5$H$_5$)$_2$(OCN)$_2$] has a structure supported by measurements other than from IR spectroscopy.[17] In our case the NCO ligand is probably N-bonded to the metal, as is its isothiocyanato-analogue, *trans*-[Mo(NCS)Cl(dppe)$_2$], the structure of which has been determined by X-ray analysis, see below. The P_L value of NCO is close to that of Cl,[18] accordingly we find that both the electrochemical behaviour of *trans*-[Mo(NCO)Cl(dppe)$_2$] and its redox potentials are quite similar to those of *trans*-[MoCl$_2$(dppe)$_2$], Table 2.

Besides dioxygen, sulphur and selenium were also found to react with solutions of compound **A** and the analogous heterocumulene complexes are isolable in reasonable yields as described in the Experimental section. Qualitatively oxygen reacts fastest with **A** and grey selenium is the slowest to react.

In the reaction with sulphur, hydrogen sulphide was detected by its odour and by reaction with lead acetate paper but its formation has not been quantified. It seems possible that the driving force for the formation of the various heterocumulene complexes is the elimination of H_2X (X = O, S or Se) but we have not studied the mechanism of these reactions. Nevertheless, as far as we are aware, these reactions and the formation of cyanide as described above and summarised by Scheme 1, are the first examples of their type.

X-Ray Crystal Structure of trans-[Mo(NCS)Cl(dppe)$_2$]: *Description of the Molecule.*—The complex molecule [Mo(NCS)Cl(dppe)$_2$] has a six-fold, distorted-octahedral, co-ordination pattern in which the chloride and thiocyanate ligand are *trans* and form an essentially linear arrangement normal to the plane of the four phosphorus atoms of the dppe ligands, Fig. 3. Selected molecular dimensions are given in Table 3. The molecule lies disordered about a crystallographic centre of symmetry and the atoms of the Cl/NCS group, particularly C(3) and Cl(4), are not well resolved; indeed, the N(3)–C(3) bond length had to be restrained towards 1.17 Å for satisfactory refinement of these atoms. The Mo atom was allowed to move away from the centre of symmetry during refinement process, but its anisotropic thermal parameters showed an unrealistic vibration ellipsoid; in the final cycles, it was constrained to stay at the centre of symmetry.

The thiocyanate ion is shown to ligate through the N atom. The N–C–S group is very close to linear, but binds to the Mo atom with an angle of 167(5)° at N(3). The bond lengths in the Cl–Mo–N–C–S unity are not very precise. Previous Mo^{II}–Cl distances are 2.432(2) Å in [Mo(CN)Cl(dppe)$_2$] (see above), 2.435(1) Å in [MoCl$_2$(dmpe)$_2$] (dmpe = Me$_2$PCH$_2$CH$_2$PMe$_2$),[19] 2.40(6) Å in [MoCl$_2$(PMe$_3$)$_4$][20] and

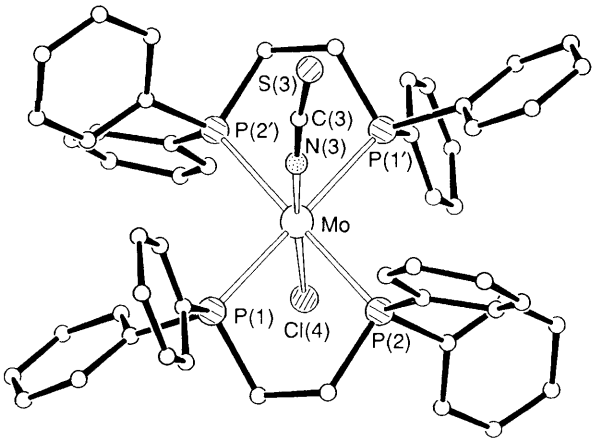

Fig. 3 A view of the X-ray crystal structure of *trans*-[Mo(NCS)Cl(dppe)$_2$]

Table 3 Selected molecular dimensions (bond lengths in Å, angles in °) in [Mo(NCS)Cl(dppe)$_2$] with e.s.d.s in parentheses

(*a*) About the Mo atom			
Mo–P(1)	2.502(4)	Mo–N(3)	1.95(3)
Mo–P(2)	2.517(4)	Mo–Cl(4)	2.664(26)
P(1)–Mo–P(2)	79.1(1)	P(2)–Mo–N(3)	93.9(14)
P(1)–Mo–N(3)	96.9(13)	P(2)–Mo–Cl(4)	84.5(4)
P(1)–Mo–Cl(4)	85.0(3)	N(3)–Mo–Cl(4)	177.3(16)
(*b*) In the thiocyanate ligand			
N(3)–C(3)	1.172(10)	Mo–N(3)–C(3)	166.9(45)
C(3)–S(3)	1.408(28)	N(3)–C(3)–S(3)	172.9(56)
(*c*) Torsion angle in the dppe ligand			
P(1)–C(1)–C(2)–P(2)	−48.4(14)		

a mean value of 2.391(5) Å in [MoCl$_2$(dppe)$_2$].[21] Octahedral molybdenum(II) complexes with thiocyanate groups appear rare, but in the molybdenum(III) complex ion [Mo(NCS)$_6$]$^{3-}$ the mean Mo–N distance is 2.088(10)[22] and in the bimetallic molybdenum(II) compounds [Mo$_2$(dppm)$_2$(NCS)$_4$] (dppm = $Ph_2PCH_2PPh_2$),[23] [Mo$_2$(NCS)$_4$(gly)$_2$] (gly = glycin) and [Mo$_2$(NCS)$_4$(ile)$_2$] (ile = isoleucin)[24] the mean Mo–N distances are 2.06(2), 2.11(1) and 2.11(1) Å. Our Mo–Cl(4) distance, 2.66(3) Å, thus looks rather longer than expected, and Mo–N(3), 1.95(3) Å, rather shorter; these suggest that the Mo atom should indeed be displaced from the crystallographic centre towards the chloride ligand.

In the diphosphine ligands there is no sign of any disorder; some of the thermal parameters are rather high, but there is no evidence for alternate orientations of the phenyl rings, significant shifts in any atom positions, or variation in the conformation of the P–C–C–P link; this last shows a normal *gauche* arrangement. The Mo–P distances, mean 2.509(8) Å, are close to those recorded for other octahedral molybdenum(II) complexes, *e.g.* 2.507(4), 2.495(9) and 2.496(3) Å in [Mo(CN)Cl(dppe)$_2$], [MoCl$_2$(dppe)$_2$][21] and [MoCl$_2$(PMe$_3$)$_4$][20] respectively.

The molecules in our crystals are discrete and separated from neighbouring molecules by normal van der Waals interactions.

Redox Potentials of the Molybdenum(II) *Derivatives.*—Cyclic voltammetry in a thf electrolyte shows that the new molybdenum(II) cyanide and heterocumulene derivatives undergo more or less reversible primary one-electron oxidation and reduction to respectively molybdenum-(III) and -(I) species. Fig. 4 illustrates a typical voltammogram for the isoselenocyanate complex. The isothiocyanate and isoselenocyanate display an accessible irreversible secondary reduction process, Fig. 4, and their voltammetric behaviour is quite analogous to that of *trans*-[MoCl$_2$(dppe)$_2$] which has been discussed in detail elsewhere.[25] Table 2 collects the primary redox potential data of the molybdenum(II) derivatives described here together with those of some closely related species that we have reported earlier.[6,7,25] It is seen that the reduction and oxidation potentials of the molybdenum(II) complexes are very dependent on the nature of the anion ligating the MoCl(dppe)$_2$ core. For the complexes listed, $E^{o\prime}(Mo^{II}–Mo^{I})$ spans a range of about 1.3 V and $E^{o\prime}(Mo^{II}–Mo^{III})$ about 1.1 V.

The anionic ligands can be classified into two distinct groups: (*i*) ligands with p_π-donor capability, NCH_2, OH and NH_2; (*ii*) ligands which are poor p_π donors, Cl, CN and the pseudo-halides (NCO, NCS and NCSe). The groups correspond well with the observed variations in the redox potentials. Where p_π donation operates an 18e configuration will be conferred on the molybdenum(II) centre and we would expect such complexes to be more difficult to reduce than the corresponding 16e systems. Table 2 shows that this is indeed the case, complexes of group (*i*) ligands are all more difficult to reduce than those of the group (*ii*) ligands. In the absence of p_π donation we would expect the oxidation to be primarily metal based and not dramatically influenced by the nature of the anionic ligand. Table 2 shows that the complexes of group (*ii*) ligands have oxidation potentials which lie in a relatively narrow range from −0.40 to −0.59 V relative the ferrocenium–ferrocene couple. In contrast, the complexes of group (*i*) ligands have redox potentials considerably more negative than those of group (*ii*) and these show a much wider variation from −0.72 to −1.51 V relative to ferrocenium–ferrocene and this is consistent with the highest-occupied molecular orbital (HOMO) in these complexes possessing considerable ligand character.

Within the complexes of group (*ii*) ligands quite clear trends in redox potentials are observed. For the pseudo-halide complexes, $E^{o\prime}(Mo^{II}–Mo^{III})$ and $E^{o\prime}(Mo^{II}–Mo^{I})$ increase with the electropositivity of the halogen in the order O < S < Se.

The separations in the oxidation and reduction potentials (ΔE, Table 2) of the pseudo-halides and the chloro-complex are very similar. The cyanide complex is substantially easier to reduce than are the other complexes of group (*ii*) ligands, presumably because it is the best π-acceptor ligand.

Electrosynthesis of an Aminocarbyne by Reduction of trans-[Mo(CN)Cl(dppe)$_2$].—We wished to determine whether the oxidation of the methyleneamide to the cyanide could be reversed by reduction in the presence of a source of protons. The primary reduction of *trans*-[Mo(CN)Cl(dppe)$_2$] becomes an irreversible two-electron process in the presence of phenol, Fig. 5(*a*) and (*b*), and the product is the aminocarbyne *trans*-[Mo(CNH$_2$)Cl(dppe)$_2$] rather than the methyleneamide, reaction (7). The evidence for this is as follows.

$$\textit{trans}\text{-[Mo(CN)Cl(dppe)}_2\text{]} \xrightarrow[2e]{\text{PhOH}} \textit{trans}\text{-[Mo(CNH}_2\text{)Cl(dppe)}_2\text{]} \quad (7)$$

Preparative controlled-potential reduction of *trans*-[Mo(CN)Cl(dppe)$_2$] in thf containing 0.2 mol dm^{-3} [NBu$_4$][BF$_4$] and 0.2 mol dm^{-3} PhOH at a mercury-pool cathode was an overall two-electron process and ^{31}P-{^1H}, ^{13}C NMR spectroscopy and cyclic voltammetry showed that a single diamagnetic product had been formed. This product was characterised as the aminocarbyne in the following way. The same complex was electrosynthesised in thf from 50% ^{13}C-enriched *trans*-[Mo(CN)Cl(dppe)$_2$] and Fig. 6 shows the ^{13}C NMR spectrum of the product in the catholyte. The ligating carbyne resonance is seen as a quintet, δ 225.9 ppm, $^2J_{PC}$ 17.2 Hz, which arises by coupling to four equivalent ^{31}P nuclei. The chemical shift and

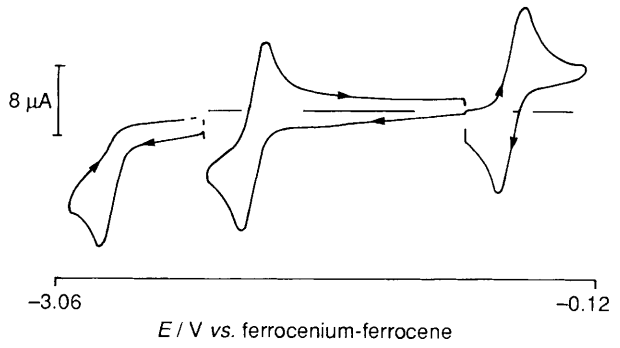

Fig. 4 Cyclic voltammogram of *trans*-[Mo(NCSe)Cl(dppe)$_2$] in thf–0.2 mol dm^{-3} [NBu$_4$][BF$_4$] at a vitreous carbon electrode, scan rate 0.1 V s^{-1}

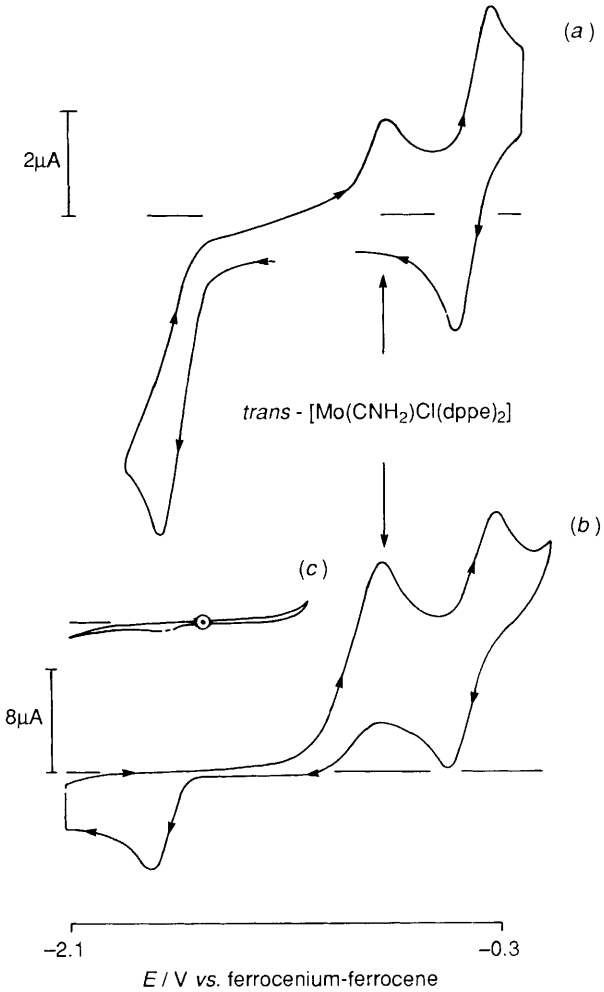

Fig. 5 Cyclic voltammograms before (*a*) and after (*b*) reduction of *trans*-[Mo(CN)Cl(dppe)$_2$] in thf–0.2 mol dm^{-3} [NBu$_4$][BF$_4$] at a mercury-pool cathode in the presence of PhOH. The voltammetry was recorded *in situ* at a platinum-wire electrode at 0.2 V s^{-1}. Notice that the current sensitivities in (*a*) and (*b*) differ by a factor of four because at the beginning of electrolysis there is a suspension of undissolved starting material; at the end of electrolysis a clear orange solution is formed; also that the cyanide reduction peak is essentially absent when the potential excursion is limited to the foot of the aminocarbyne oxidation wave (*c*); the voltammetry clearly shows that the aminocarbyne *product* oxidises to the parent cyanide (*b*).

the coupling constant are closely similar to those of the hitherto unique aminocarbyne ligand in *trans*-[Re(CNH$_2$)Cl(dppe)$_2$]$^+$, δ 222.4 ppm, $^2J_{PC}$ 13 Hz, the structure of which has been determined by X-ray analysis.[26]

Appropriately the ^{31}P-{^{1}H} NMR spectrum of the ^{13}C-

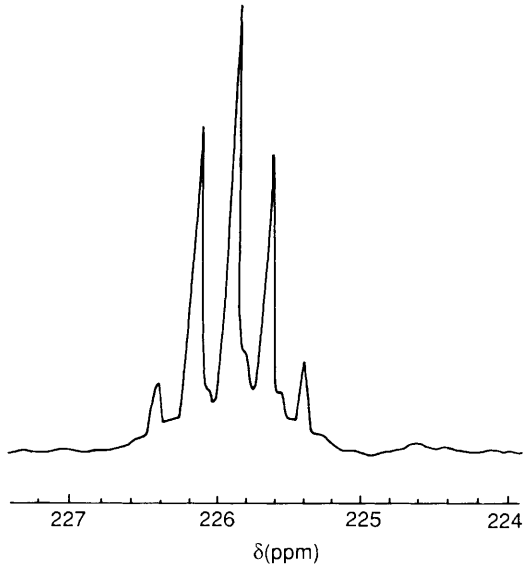

Fig. 6 ^{13}C NMR spectrum of *trans*-[Mo(CNH$_2$)Cl(dppe)$_2$] in thf–0.2 mol dm^{-3} [NBu$_4$][BF$_4$]. The spectrum is a quintet arising from coupling of the unique labelled carbyne ^{13}C to four equivalent P atoms.

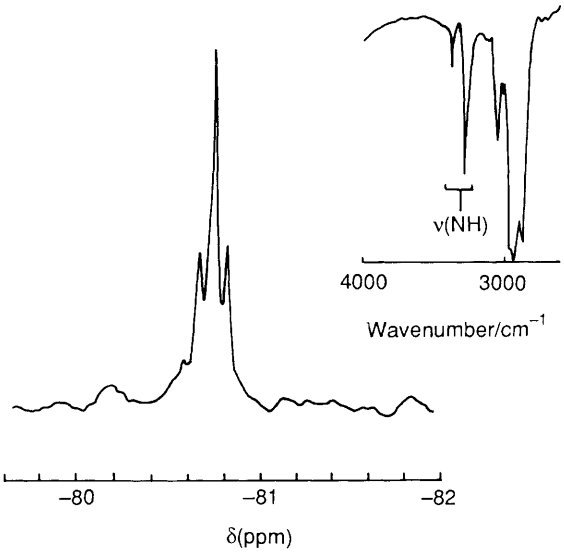

Fig. 7 The ^{31}P NMR spectrum of *trans*-[Mo(CNH$_2$)Cl(dppe)$_2$] enriched with *ca.* 50% *trans*-[Mo(^{13}CNH$_2$)Cl(dppe)$_2$]. The central peak is the singlet resonance of the unlabelled product; the superimposed doublet arises from the ^{13}C coupling of the aminocarbyne carbon to the four equivalent P nuclei. The inset shows ν(NH) for the amino-group (Nujol mull).

enriched complex shows a doublet $^2J_{PC}$ 17.2 Hz (coupling to unique [^{13}C]carbyne) and the central singlet resonance of the unlabelled material at −80.74 ppm relative to trimethyl phosphite, Fig. 7.

The IR spectrum of the isolated aminocarbyne product confirmed the presence of the amino-group and the lowering of the CN bond order: ν(NH) 3380w, 3297m, 1568m (bend) (inset in Fig. 7), ν(CN) 1396m, ν(^{13}CN) 1362 cm^{-1}.

Finally, microanalysis of the yellow product isolated on work-up of the catholyte confirmed the analytical formulation and cyclic voltammetry showed that this species was identical to that in the catholyte at the end of electrolysis. Furthermore, oxidation of the aminocarbyne regenerated the parent cyanide, Fig. 5 (*a*) and (*b*), reaction (8).

$$\textit{trans}\text{-[Mo(CNH}_2\text{)Cl(dppe)}_2\text{]} \xrightarrow[-2H^+]{-2e} \textit{trans}\text{-[Mo(CN)Cl(dppe)}_2\text{]} \quad (8)$$

$\bar{M}o{=}C{=}\overset{+}{N}H_2$ $\bar{M}o{=}\overset{+}{N}{=}CH_2$ $Mo{\equiv}\overset{+}{N}{-}\bar{C}H_2$

I II III

Fig. 8 Some canonical forms of the molybdenum aminocarbyne and methyleneamide groups

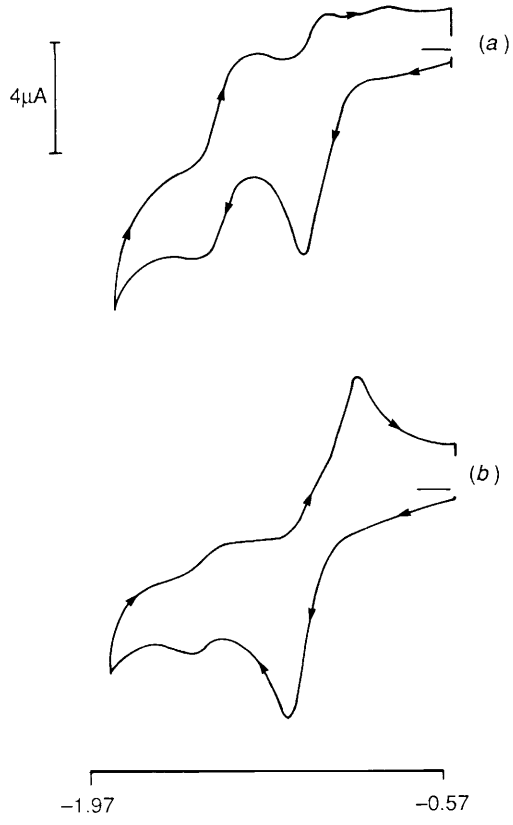

Fig. 9 Cyclic voltammetry of *trans*-[Mo(CN)Br(dppe)$_2$] in thf–0.2 mol dm^{-3} [NBu$_4$][BF$_4$] at a vitreous carbon electrode, scan rate 0.1 V s^{-1}. (*a*) Voltammetry under argon; the primary process is irreversible and leads to the formation of a quasi-reversible couple, *trans*-[Mo(CN)(thf)(dppe)$_2$].[25] (*b*) Effect of N_2 on the voltammetry; the build-up of solvato-species is suppressed and the oxidation of *trans*-[Mo(N_2)(CN)(dppe)$_2$]$^-$ is detected.

A Pathway for Isomerisation of $MoNCH_2$ *to* $MoCNH_2$ *and some Comparative Properties of these Groups.*—The oxidation of the methyleneamide to the cyanide and the reduction of this cyanide to an aminocarbyne provides a unidirectional pathway for isomerisation of the group $MoNCH_2$ to $MoCNH_2$, Scheme 2.

$$Cl\text{–}M'\text{–}NCH_2 \longrightarrow Cl\text{–}M'\text{–}CN \longrightarrow Cl\text{–}M'{\equiv}CNH_2$$

$M' = Mo(dppe)_2$

Scheme 2

The aminocarbyne complex ($E_{\frac{1}{2}}^{ox} = -0.82$ V) is about 100 mV easier to oxidise than is the methyleneamide ($E_{\frac{1}{2}}^{ox} = -0.72$ V) yet the former is apparently oxygen stable while the latter reacts extremely rapidly with O_2. This can be rationalised by supposing that the metal-based HOMO in the aminocarbyne is higher in energy than that of the amide because the contribution of canonical form **I** confers greater electron density at the metal centre of the carbyne than does the contribution of canonical form **II** to that of the amide, Fig. 8.

Conversely, positive charge on the exo-N atom of the carbyne will deter electrophilic attack, Fig. 8, whereas a significant contribution of canonical form **II** or indeed a ylide form **III** to

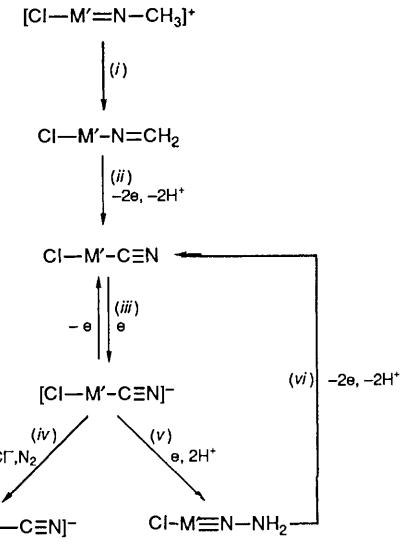

Scheme 3 M′ = Mo(dppe)$_2$: (*i*) Bu^{t}O$^-$; (*ii*) $E_p^{ox} = -0.77$ V; (*iii*) $E^{o'} = -1.79$ V; (*iv*) $E^{o'} = -2.57$ V; (*v*) PhOH; (*vi*) $E_p^{ox} = -0.87$ V

the electronic structure of the methylene amide would favour attack by electrophiles.

There is one other feature of the comparative chemistry of the two isomers which may be significant. In the polar solvent MeCN the aminocarbyne complex ionises rapidly and we have isolated *trans*-[Mo(CNH_2)(MeCN)(dppe)$_2$]Cl. This suggests that the aminocarbyne exerts a labilising effect on the Cl ligand *trans* to it, as does a nitride ligand in related complexes. In contrast, the methyleneamide complex does not appear to have a particularly labile Cl ligand. Again we can rationalise this in terms of the electron density at the metal, Fig. 8.

Electrochemical Formation of Dinitrogen Complexes.—Cyclic voltammetry of *trans*-[Mo(CN)X(dppe)$_2$], X = Cl or Br, in thf–0.2 mol dm^{-3} [NBu$_4$][BF$_4$] under an atmosphere of nitrogen shows the formation of the anionic dinitrogen complex *trans*-[Mo(N_2)(CN)(dppe)$_2$]$^-$ **D**,[27] in an overall two-electron process, reaction (9). When X = Br, the formation of **D** takes place

$$trans\text{-}[Mo(CN)X(dppe)_2] \xrightarrow[2e,-X^-]{N_2} trans\text{-}[Mo(N_2)(CN)(dppe)_2]^- \quad (9)$$

D

close to the primary reduction potential because Br$^-$ is rapidly lost from the molybdenum(I) intermediate and N_2 co-ordinates and promotes further electron transfer.[25] Fig. 9 illustrates the dramatic effect of N_2 on the voltammetry of the bromo-complex. When X = Cl the rapid formation of the dinitrogen complex occurs after reduction of the anionic intermediate *trans*-[Mo(CN)Cl(dppe)$_2$]$^-$ and this reflects the relative ease of cleavage of the Mo^I–X bond.[25]

Conclusions

The chemistry and electrochemistry described in this paper are summarised by Schemes 1 and 3. Here we make some further observations.

First, the reduction of Mo–C≡N to Mo≡C–NH_2 provides a chemical precedent for a possible role for ligating aminocarbyne in the biological reduction of aqueous cyanide by molybdenum nitrogenase.[28,29] The enzymatic reduction gives the four-electron product methylamine and the six-electron products ammonia and methane. We have shown that the methylene-amide lies on a four-electron pathway to methylamine; whether or not the aminocarbyne lies on a six-electron pathway to ammonia and methane remains to be studied.

Secondly, the N atom in the methylimide complexes can be introduced from molecular nitrogen *via* reactions at the $Mo(dppe)_2$ assembly, thus the reactions outlined in Schemes 1 and 3 should provide a means of extending the range of N-containing products that can be made under mild conditions from N_2.

Experimental

General.—Solvents were freshly distilled under dinitrogen from an appropriate drying agent using standard laboratory methods. Solvent, electrolytes and complexes were generally handled under an inert atmosphere using Schlenk techniques. The complex *trans*-[Mo(NMe)Cl(dppe)$_2$]I and its $^{13}CH_3$ analogue were synthesised from *trans*-[MoN(Cl)(dppe)$_2$] and MeI (or $^{13}CH_3I$) as described elsewhere. Microanalyses were by Mr. C. J. Macdonald of the AFRC Nitrogen Fixation Laboratory, University of Sussex.

Instruments.—Electrochemical measurements were made using a Hi-Tek Instruments type DT-101 potentiostat and type PPR1 waveform generator. Voltammograms were recorded on a Philips PM 8043 X-Y recorder and charge was measured using a Chemical Electronics integrator.

IR spectra were recorded on a Bio-Rad FTIR type 3240 SPC spectrometer and NMR spectra using a JEOL FX-90G instrument.

Preparation of Compounds.—*trans*-[Mo(NCH$_2$)Cl(dppe)$_2$]. The complex *trans*-[Mo(NMe)Cl(dppe)$_2$]I (0.13 g, 0.12 mmol) was suspended in thf (30 cm^3) and K[OBu^t] (0.043 g, 0.35 mmol) was added; the solution changed from pink to yellow-brown. Diethyl ether (20 cm^3) was added, and a small amount of insoluble material was removed by filtration. The clear solution was taken to dryness, and the solid product was washed with degassed water (6 cm^3 × 3), collected by filtration, washed with a small amount of diethyl ether (4 cm^3 × 2) and dried *in vacuo*. Yield = 0.06 g, 0.062 mmol (52%) [Found: C, 65.0; H, 5.4; N, 1.3. Calc. for $C_{53}H_{52}ClMoNOP_4$ (A·H$_2$O): C, 65.3; H, 5.4; N, 1.4].

trans-[Mo(CN)Cl(dppe)$_2$]. *Method 1.* The complex *trans*-[Mo(NMe)Cl(dppe)$_2$]I (0.54 g, 0.50 mmol) was suspended in thf (30 cm^3) then K[OBu^t] (0.18 g, 1.47 mmol) was added. The solution immediately changed to yellow-brown. The addition of iodine (0.14 g, 0.55 mmol) afforded a yellow suspension of the product. After 10 min of stirring the volume of the solution was reduced to *ca.* 5 cm^3. The product was collected by filtration, and washed with thf (3 cm^3 × 3) then water (8 cm^3 × 5). It was finally washed with pentane (3 cm^3 × 3) and dried *in vacuo*. Yield = 0.31 g, 0.325 mmol (65%).

Method 2. Tetrabutylammonium cyanide (0.26 g, 0.97 mmol) was added under an atmosphere of dry dinitrogen to a suspension of *trans*-[Mo(N$_2$)$_2$(dppe)$_2$] (0.95 g, 0.96 mmol) in thf (50 cm^3). The orange solid rapidly dissolved and the solution acquired the dark red colour of *trans*-[Mo(N$_2$)(CN)(dppe)$_2$]$^-$.[27] After stirring overnight at room temperature, benzyl chloride (2 cm^3) was added and the solution was warmed to *ca.* 40 °C for 5 min whereupon a yellow product deposited from solution. The solution was stirred for 1 h, cooled and the yellow solid was filtered off, washed with cold thf (5 cm^3) and dried *in vacuo*. The spectroscopic and voltammetric properties of the product were identical with those of the cyanide prepared by method 1. Yield = 0.9 g, 0.94 mmol (98%) (Found: C, 65.5; H, 5.9; N, 1.5. Calc. for $C_{53}H_{48}ClMoP_4$: C, 66.7; H, 5.1; N, 1.5%).

trans-[Mo(CN)Br(dppe)$_2$]. The complex *trans*-[Mo(N$_2$)$_2$(dppe)$_2$] (0.8 g, 0.81 mmol) was dissolved in thf (50 cm^3), [NBu$_4$][CN] (0.3 g, 0.59 mmol) was added and the solution was stirred overnight. Degassed 1,5-dibromopentane (180 μl) was then added and the mixture irradiated with a tungsten light (275 W) for 1 h. During this period the solution changed from dark red to dark orange. A little solid was removed by filtration and the volume of the filtrate was reduced to *ca.* 10 cm^3. The solution was stored at −15 °C for 1 h, during which time the product precipitated as a yellow solid. It was removed by filtration and dried *in vacuo*. Yield = 0.42 g, 0.42 mmol (52%) (Found: C, 63.8; H, 5.5; N, 1.3. Calc. for $C_{53}H_{48}BrMoNP_4$: C, 63.7; H, 4.8; N, 1.4%).

trans-[Mo(NCO)Cl(dppe)$_2$]. The complex *trans*-[Mo(NMe)Cl(dppe)$_2$]PF$_6$ (0.49 g, 0.44 mmol) was suspended in thf (40 cm^3), K[OBu^t] (0.16 g, 1.33 mmol) was added and the solution changed to orange-brown. It was flushed with dry dioxygen (**CAUTION**: peroxides) until the colour changed to a bright yellow, whereupon the solvent was evaporated to dryness. The yellow solid was washed with water (10 cm^3 × 5), then with pentane and dried *in vacuo*. It was purified by dissolving in thf (15 cm^3) and removing undissolved products by filtration followed by the addition of diethyl ether (10 cm^3) to the filtrate. This afforded yellow crystals which were collected by filtration and dried *in vacuo*. Yield = 0.26 g, 0.27 mmol (60%) (Found: C, 66.5; H, 5.2; N, 1.4. Calc. for $C_{57}H_{48}ClMoNOP_4$: C, 65.6; H, 5.0; N, 1.4%).

trans-[Mo(NCS)Cl(dppe)$_2$]. Potassium *tert*-butoxide (0.17 g, 1.38 mmol) was added to a suspension of *trans*-[Mo(NMe)Cl(dppe)$_2$]I (0.53 g, 0.49 mmol) in thf (40 cm^3). To the yellowish brown solution was added suphur (0.09 g, 0.294 mmol) and the resultant red solution stirred for 2 h. The solvent was then evaporated to dryness *in vacuo* and product was washed with water (7 × 20 cm^3) and dried. The residue crystallised from thf–hexane as an orange crystalline solid and was dried *in vacuo*. Yield = 0.2 g, 0.21 mmol (42%) (Found: C, 64.1; H, 5.2; N, 1.2. Calc. for $C_{53}H_{48}ClMoNP_4S$: C, 64.5; H, 4.9; N, 1.4%).

trans-[Mo(NCSe)Cl(dppe)$_2$]. Potassium *tert*-butoxide (0.21 g, 1.7 mmol) was added to a suspension of *trans*-[Mo(NMe)Cl(dppe)$_2$]PF$_6$ (0.66 g, 0.61 mmol) in thf (45 cm^3). The solution became yellowish brown, and selenium (0.069 g, 0.79 mmol) was added. The resultant solution was stirred overnight and then filtered through Celite to remove the unreacted selenium; solvent was removed to produce a light brown solid. Repeated washing of the brown solid with water (7 × 15 cm^3) gave the final yellow product, which was dried *in vacuo* and recrystallised from thf–hexane as bright yellow prisms. Yield = 0.29 g, 0.28 mmol (46%) (Found: C, 61.0; H, 5.0; N, 1.2. Calc. for $C_{53}H_{48}ClMoNP_4Se$: C, 61.6; H, 4.7; N, 1.4%).

Electrosynthesis of trans-[Mo(CN)Cl(dppe)$_2$]. The complex *trans*-[Mo(NMe)Cl(dppe)$_2$]PF$_6$ (0.256 g, 0.23 mmol) was suspended in the thf electrolyte contained in the electrolysis cell under dinitrogen. The salt K[OBu^t] (0.085 g, 0.70 mmol) was then added to this solution, the colour changing from mauve to orange-yellow and the suspension dissolved. The electrolysis was performed at *ca.* −0.7 V *versus* ferrocenium–ferrocene. During the course of the electrolysis the solution changed from orange-yellow to brown-green but fouling of the electrode caused considerable problems. After the current had decayed to about 5% of its initial value the anolyte solution was transferred to a Schlenk flask and some material, probably KPF_6, was removed by filtration through Celite. The solution was taken to dryness and the residue, a green-brown solid, was dissolved in methanol (*ca.* 15 cm^3). The solution was filtered through Celite to remove further insoluble material and the volume of filtrate was reduced to about 8 cm^3. It was stored at −15 °C for 2 d whereby a mixture of small mauve needles (starting material) and large green prisms of *trans*-[Mo(CN)Cl(dppe)$_2$]·MeOH deposited. The green crystals were separated for X-ray analysis. When crushed they yield a yellow powder.

trans-[Mo(CNH$_2$)Cl(dppe)$_2$]. The complex *trans*-[Mo(CN)Cl(dppe)$_2$] (0.15 g, 0.159 mmol) was suspended in the electrolyte under dinitrogen. Phenol (0.50 g, 5.39 mmol) was added to this solution. Electrolysis was performed at *ca.* −1.5 V. After the consumption of about 2F mol^{-1} all the suspended solid had dissolved, an orange solution was produced and the current had

Table 4 Final atomic coordinates (fractional × 10^4) for [Mo(CN)Cl(dppe)$_2$]·MeOH with e.s.d.s in parentheses

Atom	*x*	*y*	*z*	Atom	*x*	*y*	*z*
Mo	2200.8(2)	1747.4(3)	4841.7(3)	C(35a)	−365(4)	2744(4)	6082(5)
C(11a)	2907(4)	1586(3)	7057(3)	C(36a)	2(3)	2716(3)	5442(4)
C(12a)	2124(4)	1686(3)	7186(3)	C(31b)	1596(4)	3942(3)	4563(3)
C(13a)	1937(5)	1412(4)	7880(5)	C(32b)	2366(4)	4150(4)	4517(4)
C(14a)	2502(6)	1018(5)	8442(4)	C(33b)	2561(5)	4934(5)	4426(4)
C(15a)	3266(6)	915(5)	8313(5)	C(34b)	1998(6)	5490(4)	4383(4)
C(16a)	3471(4)	1193(4)	7631(4)	C(35b)	1228(5)	5295(4)	4440(4)
C(11b)	3482(4)	2994(3)	6490(4)	C(36b)	1023(4)	4531(4)	4514(3)
C(12b)	3990(4)	3410(4)	6094(4)	P(3)	1304.3(8)	2936.0(8)	4673.8(8)
C(13b)	4215(5)	4160(5)	6319(5)	C(3)	499(3)	2821(3)	3744(3)
C(14b)	3958(5)	4508(4)	6927(6)	C(4)	361(3)	1967(3)	3478(3)
C(15b)	3466(4)	4121(5)	7328(5)	P(4)	1332.6(8)	1488.6(8)	3482.8(8)
C(16b)	3232(4)	3351(4)	7112(4)	C(41a)	1659(3)	1914(3)	2625(3)
P(1)	3143.3(8)	2013.8(8)	6156.9(8)	C(42a)	1136(3)	2287(4)	2016(4)
C(1)	4113(3)	1568(3)	6075(3)	C(43a)	1415(5)	2607(4)	1378(4)
C(2)	3996(3)	715(3)	5818(3)	C(44a)	2209(5)	2551(4)	1361(4)
P(2)	3088.8(8)	560.2(8)	4982.2(8)	C(45a)	2725(4)	2164(4)	1948(4)
C(21a)	2769(3)	−399(3)	5253(3)	C(46a)	2462(3)	1847(4)	2585(3)
C(22a)	3315(4)	−992(4)	5504(4)	C(41b)	1027(3)	502(3)	3136(3)
C(23a)	3085(5)	−1705(4)	5754(4)	C(42b)	1292(3)	158(3)	2508(4)
C(24a)	2293(6)	−1838(4)	5727(4)	C(43b)	1087(4)	−597(4)	2277(4)
C(25a)	1733(5)	−1281(5)	5449(5)	C(44b)	609(4)	−1026(4)	2674(4)
C(26a)	1972(4)	−573(4)	5224(4)	C(45b)	339(4)	−698(4)	3293(4)
C(21b)	3539(3)	331(3)	4134(3)	C(46b)	549(3)	58(3)	3526(3)
C(22b)	4197(4)	739(4)	3986(4)	Cl(5)	1109.5(8)	1157.8(8)	5359.7(9)
C(23b)	4496(5)	614(6)	3320(6)	C(6)	3136(3)	2329(3)	4380(3)
C(24b)	4145(6)	69(7)	2780(5)	N(6)	3619(4)	2609(3)	4184(3)
C(25b)	3498(6)	−356(5)	2900(4)				
C(26b)	3186(4)	−222(4)	3581(4)				
C(31a)	742(3)	3053(3)	5469(3)	Methanol molecule			
C(32a)	1118(4)	3436(3)	6165(3)	C(7)	5508(7)	3556(7)	4511(7)
C(33a)	749(5)	3455(4)	6810(4)	O(7)	5267(4)	2862(5)	4124(5)
C(34a)	22(5)	3093(4)	6771(5)	H(7)	4547(53)	2710(44)	4121(43)

decayed to a low level. The anolyte was transferred to a Schlenk flask, the solution was evaporated to dryness and methyl cyanide (18 cm^3) was added. The yellow product *trans*-[Mo(CNH$_2$)Cl(dppe)$_2$] was removed by filtration and dried *in vacuo*. Yield = 0.02 g, 0.021 mmol (13%) (Found: C, 66.1; H, 5.8; N, 1.0. Calc. for $C_{53}H_{50}ClMoNP_4$: C, 66.6; H, 5.3; N, 1.5%).

The filtrate was kept in the freezer overnight, and crystalline dark brown *trans*-[Mo(CNH$_2$)(MeCN)(dppe)$_2$]Cl deposited. It was filtered off and dried *in vacuo*. Yield = 0.08 g, 0.08 mmol (51%) (Found: C, 66.8; H, 5.8; N, 2.6. Calc. for $C_{55}H_{53}ClMoN_2P_4$: C, 66.1; H, 5.3; N, 2.8%).

Crystal-structure Analysis of [Mo(CN)Cl(dppe)$_2$]·MeOH.—*Crystal data.* $C_{53}H_{48}ClMoNP_4{\cdot}CH_4O$, M = 986.3, monoclinic, space group $P2_1/n$ (equivalent to no. 14), a = 16.87(1), b = 17.155(2), c = 17.116(3) Å, β = 102.63(1)°, U = 4833.9 Å^3, Z = 4, D_c = 1.355 g cm^{-3}, $F(000)$ = 2040, μ(Mo-Kα) = 4.9 cm^{-1}, λ(Mo-Kᾱ) = 0.710 69 Å.

Crystals are dark green, irregular lumps and are air-sensitive. One, *ca.* 0.33 × 0.38 × 0.48 mm, was sealed in a glass capillary and photographed to check the crystal quality and for preliminary cell parameters. On our Enraf-Nonius CAD4 diffractometer (with monochromated Mo-Kα radiation) accurate cell dimensions were determined from the settings of 25 reflections (θ = 10–11°) each centred in four orientations, and diffraction intensities were measured to θ_{max} = 20°. Two reflections monitored throughout the data collection showed steady deterioration to *ca.* 66% of their initial intensities; a deterioration factor was applied accordingly. Corrections for Lorentz-polarisation effects and to eliminate negative intensities (by Bayesian statistical methods) were also applied. No absorption correction was made; the crystal had decayed too much for meaningful ψ-scan measurements to be made and the low absorption coefficient suggests that very little correction was necessary.

Of the 4506 unique data recorded at 293 K, 3574 had $I > 2\sigma_I$ and were used in the structure determination by automated Patterson methods (using the routine PATT in the program SHELXS).[30] Most of the structure was clear from the Fourier maps produced; the remaining atoms were located in difference syntheses. Hydrogen atoms in the diphosphine ligands and in the methyl group of the methanol molecule were included in idealised positions (C–H 0.98 Å) and their isotropic thermal parameters were set to ride on those of their bonded carbon atoms. The hydroxyl hydrogen atom of the solvent molecule was located in a difference map and was refined independently and satisfactorily. Refinement, by large-block-matrix least-square methods, was achieved with an extended version of SHELX 76,[31] and converged at R = 0.048, R' = 0.047 for 4099 reflections (those with $I > \sigma_I$) weighted $w = (\sigma_F^2 + 0.000\,76F^2)^{-1}$. In a final difference map, the highest peaks, *ca.* 0.8 e Å^{-3}, were all close to the Mo atom. Final atomic coordinates are in Table 4.

Crystal-structure Analysis of [Mo(NCS)Cl(dppe)$_2$].—*Crystal data.* $C_{53}H_{48}ClMoNP_4S$, M = 986.3, triclinic, space group $I\bar{1}$ (equivalent to no. 2), a = 10.642(1), b = 14.446(1), c = 15.968(1) Å, α = 75.516(8), β = 86.631(7), γ = 82.957(8)°, U = 2357.9 Å^3, Z = 2, D_c = 1.389 g cm^{-3}, $F(000)$ = 1016, μ(Mo-Kα) = 5.4 cm^{-1}, λ(Mo-Kᾱ) = 0.710 69 Å.

Crystals were small, yellow, rhombic prisms. One, *ca.* 0.12 × 0.05 × 0.05 mm, was mounted in air on a glass fibre. In a routine similar to that described above, cell parameters were determined from the goniometer settings of 20 reflections having θ in the range 7.5–11.0°, and diffraction intensities were measured to θ_{max} = 20°. The data were corrected similarly for Lorentz-polarisation effects and to ensure no negative intensities. No correction for deterioration was necessary and, considering the small size of the crystal and the calculated

Table 5 Final atomic coordinates (fractional × 10^4) for [Mo(NCS)Cl(dppe)$_2$] with e.s.d.s in parentheses

Atom	*x*	*y*	*z*
Mo	0	0	0
C(11a)	2235(16)	1602(11)	411(9)
C(12a)	3521(17)	1616(15)	469(11)
C(13a)	4160(19)	2366(17)	41(13)
C(14a)	3488(24)	3166(19)	−451(13)
C(15a)	2181(25)	3174(18)	−531(12)
C(16a)	1601(20)	2383(17)	−93(13)
C(11b)	823(15)	852(10)	1988(9)
C(12b)	−284(15)	544(11)	2375(11)
C(13b)	−675(15)	694(11)	3177(11)
C(14b)	64(19)	1170(11)	3583(11)
C(15b)	1188(19)	1442(13)	3199(12)
C(16b)	1575(15)	1340(10)	2403(11)
P(1)	1367(4)	598(3)	929(3)
C(1)	2592(14)	−397(12)	1310(10)
C(2)	3266(13)	−743(14)	555(10)
P(2)	2103(4)	−933(3)	−208(3)
C(21a)	2106(13)	−2238(12)	25(13)
C(22a)	2543(18)	−2843(19)	801(13)
C(23a)	2536(20)	−3816(21)	966(16)
C(24a)	2061(18)	−4231(15)	391(16)
C(25a)	1600(15)	−3637(17)	−372(14)
C(26a)	1607(13)	−2657(16)	−549(13)
C(21b)	3036(14)	−619(19)	−1195(11)
C(22b)	3246(18)	310(19)	−1547(14)
C(23b)	3966(25)	605(27)	−2267(18)
C(24b)	4578(24)	−66(28)	−2698(16)
C(25b)	4371(19)	−978(24)	−2371(16)
C(26b)	3594(17)	−1305(16)	−1655(13)
N(3)	203(45)	1008(29)	−1052(21)
C(3)	94(46)	1578(30)	−1717(23)
S(3)	77(13)	2187(9)	−2556(8)
Cl(4)	−257(16)	−1438(16)	1394(15)

absorption coefficient, no absorption correction was applied. 2192 Unique data collected at 293 K were input to the SHELX program system.

In the non-centrosymmetric space group *I*1, an electron-density map phased by a Mo atom and subsequent difference maps yielded clearly the Mo(dppe)$_2$ moiety; the remaining atoms were not resolved and appeared disordered. Refinement indicated that the structure is in fact centrosymmetric (space group $I\bar{1}$) with the Mo at (or very close to) a centre of symmetry and with random disorder of the Cl and NCS ligands. It was necessary to restrain the N–C bond towards 1.17 Å in the refinement process.

Hydrogen atoms in the dppe ligands were included in idealised positions (C–H 0.98 Å) but with independent isotropic thermal parameters. All the non-hydrogen atoms, except for the N and C atoms in the thiocyanate ligand, were allowed anisotropic thermal parameters. Refinement, by full-matrix least-squares methods, was concluded with $R = 0.067$ and $R_g = 0.060$[31] for 1272 reflections (those having $I > 1.5\sigma_I$) weighted $w = \sigma_F^{-2}$. There were no peaks of significance in the final difference maps; all features were between −0.39 and 0.42 e Å^{-3}. Final atomic coordinates are given in Table 5.

For both X-ray analyses, scattering factors for neutral atoms were taken from ref. 32. Computer programs used in the analyses have been noted above and in Table 4 of ref. 33, and were run on the DEC-MicroVAX II computer in this laboratory.

Additional material available from the Cambridge Crystallographic Data Centre comprises H-atom coordinates, thermal parameters and remaining bond lengths and angles.

References

1 C. J. Pickett and J. Talarmin, *Nature (London)*, 1985, **317**, 652.
2 C. J. Pickett, K. S. Ryder and J. Talarmin, *J. Chem. Soc., Dalton Trans.*, 1986, 1453.
3 C. J. Pickett and G. J. Leigh, *J. Chem. Soc., Chem. Commun.*, 1981, 1033.
4 W. Hussain, G. J. Leigh and C. J. Pickett, *J. Chem. Soc., Chem Commun.*, 1982, 747.
5 C. J. Pickett, K. Cate, C. J. Macdonald, M. Y. Mohammed, K. S. Ryder and J. Talarmin, *Nitrogen Fixation: Hundred Years After*, eds. H. Bothe, F. J. de Bruijn and W. E. Newton, G. Fischer, Stuttgart, 1988, pp. 51–56.
6 M. Y. Mohammed and C. J. Pickett, *J. Chem. Soc., Chem. Commun.*, 1988, 1191.
7 D. L. Hughes, M. Y. Mohammed and C. J. Pickett, *J. Chem. Soc., Chem. Commun.*, 1988, 1481.
8 D. L. Hughes, D. J. Lowe, M. Y. Mohammed, C. J. Macdonald and C. J. Pickett, *Polyhedron*, 1989, **8**, 1653.
9 C. J. Pickett and K. S. Ryder, unpublished work.
10 C. J. Pickett, J. E. Tolhurst, A. Copenhauer, T. A. George and R. K. Lester, *J. Chem. Soc., Chem. Commun.*, 1982, 1071; C. J. Pickett and K. S. Ryder, *J. Chem. Soc., Chem. Commun.*, 1988, 1364.
11 D. L. Hughes, M. Y. Mohammed and C. J. Pickett, *J. Chem. Soc., Chem. Commun.*, 1989, 1399.
12 J. Chatt, R. J. Dosser and G. J. Leigh, *J. Chem. Soc., Chem Commun.*, 1972, 1243.
13 B. F. G. Johnson, B. L. Haymore and J. R. Dilworth, in *Comprehensive Coordination Chemistry*, eds. G. Wilkinson, R. D. Gillard and J. A. McCleverty, Pergamon, Oxford, 1987, vol. 2, p. 125.
14 J. Chatt, R. A. Head, G. J. Leigh and C. J. Pickett, *J. Chem. Soc., Dalton Trans.*, 1979, 1638.
15 A. H. Norbury, *Adv. Inorg. Chem. Radiochem.*, 1975, **17**, 232.
16 K. Vrieze and G. van Koten, in *Comprehensive Coordination Chemistry*, eds. G. Wilkinson, R. D. Gillard and J. A. McCleverty, Pergamon, Oxford, 1987, vol. 2, p. 225.
17 W. Beck and W. P. Fehlhammer, *Int. Rev. Sci., Inorg. Chem., Ser. 1*, 1972, **2**, 253.
18 J. Chatt, C. T. Kan, G. J. Leigh, C. J. Pickett and D. R. Stanley, *J. Chem. Soc., Dalton Trans.*, 1980, 2032.
19 L. K. Fong, J. R. Fox, B. M. Foxman and N. J. Cooper, *Inorg. Chem.*, 1986, **25**, 1880.
20 E. Carmona, J. M. Marin, M. L. Poveda, J. L. Atwood and R. D. Rogers, *Polyhedron*, 1983, **2**, 185.
21 M. Nardelli, G. Pellizzi and G. Predieri, *Gazz. Chim. Ital.*, 1980, **110**, 375.
22 J. R. Knox and K. Eriks, *Inorg. Chem.*, 1968, **7**, 84.
23 E. H. Abbott, K. S. Bose, F. A. Cotton, W. T. Hall and J. C. Sekutowski, *Inorg. Chem.*, 1978, **17**, 3240.
24 A. Bino and F. A. Cotton, *Inorg. Chem.*, 1979, **18**, 1381.
25 T. I. Al-Salih and C. J. Pickett, *J. Chem. Soc., Dalton Trans.*, 1985, 1255.
26 A. J. L. Pombeiro, D. L. Hughes, C. J. Pickett and R. L. Richards, *J. Chem. Soc., Chem. Commun.*, 1986, 246.
27 J. Chatt, G. J. Leigh, H. Neukomm, C. J. Pickett and D. R. Stanley, *J. Chem. Soc., Dalton Trans.*, 1980, 121.
28 J.-G. Li, B. K. Burgess and J. L. Corbin, *Biochemistry*, 1982, **21**, 4393.
29 D. J. Lowe, K. Fisher, R. N. F. Thorneley, S. A. Vaughn and B. K. Burgess, *Biochemistry*, 1989, **28**, 8460.
30 G. M. Sheldrick, in *Crystallographic Computing 3*, eds. G. M. Sheldrick, C. Krüger and R. Goddard, Oxford University Press, 1985, p. 175.
31 G. M. Sheldrick, SHELX 76, Program for crystal structure determination, University of Cambridge, 1976.
32 *International Tables for X-Ray Crystallography*, Kynoch Press, Birmingham, 1974, vol. 4, pp. 99 and 149.
33 S. N. Anderson, R. L. Richards and D. L. Hughes, *J. Chem. Soc., Dalton Trans.*, 1986, 245.

Received 21*st June* 1990; *Paper* 0/02779K